

Long-Term Heat Storage in the Great Lakes

THOMAS E. CROLEY II

Great Lakes Environmental Research Laboratory, Environmental Research Laboratories, National Oceanic and Atmospheric Administration, U.S. Department of Commerce, Ann Arbor, Michigan

Practical estimation of long-term daily Great Lakes evaporation requires one-dimensional (depth) models of heat storage and mixing. Conceptual models are preferable to physical models for small-computer simulations that are multiple, continuous, and long. This paper describes a new conceptual superposition model of heat storage to extend an existing evaporation model along the lake depth. The resulting daily model is recalibrated to remotely sensed surface water temperatures and is used to illustrate anew seasonal heating and cooling cycles, heat-temperature hysteresis, water column turnovers, and mixed-layer developments. It is used as well to compare the vertical distribution of temperatures with independent bathythermograph data. The time occurrence structure of evaporation on the Great Lakes is investigated, and the effects of summertime initial conditions on subsequent wintertime behavior of evaporation are simulated. Impacts of perceived large-lake thermodynamic behavior are analyzed, and suggestions are made for further research.

INTRODUCTION

Estimation of daily evaporation over long time periods opens possibilities for understanding important physical processes that involve lake evaporation. Water supply forecasts and lake level outlooks can be improved to better utilize the long-term memory of heat storage in the lakes. It is already apparent that heat storages in the Great Lakes have longer half-lives than overland moisture storages in the basins. Water balance computations of groundwater become possible where before groundwater was ignored so that evaporation could be estimated. Lake effect snowfall may be better related, through appropriate mesoscale atmospheric models, to lake heat storage.

There is much potential insight to be gained from long-term daily evaporation simulations when considering physical systems that "remember," via heat or mass storage, earlier meteorological inputs at time lags of months to years. Daily data are readily available for both historical simulations and near real-time extended outlooks of lake evaporation. We often want to simulate 40-50 years continuously for exploration of daily evaporation, heat fluxes, and ice dynamics on the Great Lakes, as well as to make numerous variable period outlooks of the order of 1 month, 6 months, and more than a year. We want to be able to use both simulation and forecasting models "in the field," at the operating or regulating agency level, on small machines likely to be in place or easily obtained. Thus Great Lakes hydrological researchers often need multiple, continuous simulations of lake evaporation over long time periods at a daily time interval, and these simulations must be performable on small computers.

Daily and monthly evaporation from the Laurentian Great Lakes have been estimated in a variety of manners with little verification because evaporation is not measurable for such large areas and because back calculations of evaporation from water balances are fraught with objectionable levels of error in measurement or error in assumption of other quantities. Comprehensive heat balances with direct and indirect heat flux measurements were made on Lake Ontario during

the International Field Year on the Great Lakes [Derecki, 1981; Phillips, 1978; Pinsak and Rodgers, 1981] and on Lakes Superior and Erie [Richards and Irbe, 1969; Schertzer, 1978, 1987]; these have been used to estimate evaporation. Researchers have utilized recently available water surface temperature data, remotely sensed through aircraft and satellites, in their evaporation estimates [Atmospheric Environment Service, 1988] and, finally, to calibrate lumped thermodynamic models for each lake [Croley, 1989a].

While these models comprise our best evaporation estimators for continuous-time simulations over several years or more, work remains to be done to better represent lake heat storage and mechanical mixing. Better heat storage and mixing models allow extension of deep lake evaporation models to shallow lakes, extension of existing point models of lake thermodynamics to one dimension throughout the lake depth, comparison of temperature-depth profiles to completely independent measurements over several years of continuous simulation, and better depiction and understanding of the long-term seasonal evaporation and thermodynamics cycles of large lakes. They also allow specific looks at related long-term thermodynamic and atmospheric processes. Either existing physical models or new conceptual models may be used for heat storage and mixing in the hydrological computation of evaporation.

The state of the art in one-dimensional physical models of lake heat storage and mixing is good at the synoptic to seasonal time scale [McCormick and Meadows, 1988]. Current models accurately describe summertime heating and mixed-layer development, and simple convective adjustments alone work satisfactorily in many cases for fall, winter, and diurnal surface cooling; a small eddy diffusivity can be added for background and deep mixing (M. McCormick, personal communication, 1991). However, available physical models typically require higher frequency data than are available for the long term, and the daily data frequency of extended hydrologic studies is too low to describe vertical mixing adequately with physics. Physical models can become complicated with the consideration of boundaries, including the lake bottom in water temperature-depth profile development. Physical models also require numerical solu-

This paper is not subject to U.S. copyright. Published in 1992 by the American Geophysical Union.

Paper number 91WR02500.

tions with concerns for unstable solution schemes and for incorrectly converging solutions (because of incomplete physical descriptions or numerical error, often requiring heuristic corrections). Physical models, at a 15-min time step, increase computations by two orders of magnitude over daily hydrological models, and each iteration can be more computation intensive depending on the numerical solution. Thus available physical heat storage and mixing models are not suitable for hydrologic simulations for a variety of reasons.

The intended uses for hydrological models thus dictate the incorporation of conceptual rather than physical models to describe heat storage and mixing in a lake. A conceptual mixing model may be combined with a comprehensive heat balance through superposition heat storage for use with available daily data in any size lake. Instabilities in resulting temperature-depth profiles cannot develop as in numerical solutions to physical models; superposition of profiles, their mixing, and their subsequent evolution guarantee both that stable profiles develop which recognize the mixing layer concept and that stable, physically satisfying, density stratifications are always represented. The model should replicate data and physical interpretations on time scales greater than the daily, including low-frequency growth of the mixed layer, turnover timing, vertical temperature distributions, seasonal heat fluxes and heat in storage, water surface temperatures, and long-term lake water balances.

This paper expands earlier work [Croley, 1989a] on a point evaporation model to a one-dimensional thermodynamics model by introducing a conceptual heat storage superposition model that explicitly recognizes lake storage capacity. The resulting model is recalibrated, verified, and used to depict and interpret heat storage and evaporation behavior and to determine the nature of evaporation occurrences on the Great Lakes. Finally, a simulation is conducted to understand how increased heat storage amounts are dissipated and what their consequences may be.

GREAT LAKES EVAPORATION MODEL

The heat added to a lake in a day is given by a simple energy balance:

$$\Delta H = A_w(Q_i - Q_r + Q_l - Q_e + Q_h + Q_p)d + A_i(Q_i - Q'_r + Q'_l - Q'_e + Q'_h + Q'_p)d + I - O \quad (1)$$

where ΔH is heat addition in a day, A_w and A_i are the areas of the open water surface and ice surface, respectively, Q_i is the daily average rate of incident shortwave radiation to a unit area, Q_r and Q'_r are the unit average reflected shortwave radiation rates to the water and ice, Q_l and Q'_l are the unit average net longwave radiation exchange rates, Q_e and Q'_e are the unit average latent heat transfer rates, Q_h and Q'_h are the unit average sensible heat transfer rates, Q_p and Q'_p are the unit average overwater precipitation heat advection rates, d is day, I is daily inflow heat advection, and O is daily outflow heat advection. The latent heat rate is given by the aerodynamic equation, and the sensible heat rate may be given through use of Bowen's ratio:

$$Q_e = \Theta r C_E (q_w - q) U \quad (2)$$

$$Q_h = B Q_e \quad (3)$$

where Θ is latent heat of vaporization, r is density of air, C_E is bulk evaporation coefficient, q_w is saturation specific humidity at surface temperature, q is specific humidity of the atmosphere, U is wind speed, and B is Bowen's ratio. Overice values, Q'_e and Q'_h , are also given by (2) and (3) but evaluated using the latent heat of sublimation and temperatures, specific humidities, and Bowen's ratio over ice.

Croley [1989a, b] combined use of the aerodynamic equation, determining mass transfer coefficients through stability considerations [Quinn, 1979], with lumped concepts of classical energy conservation, as in (1), with contemporary expressions of water surface heat fluxes and with a heat storage model for large lakes. Overwater meteorology was estimated from nearby overland values by applying overwater corrections [Phillips and Irbe, 1978], and Bowen's ration was determined separately; ice cover was estimated empirically independent of the heat balance [Assel, 1983a]. Note that

$$Q_h = r C_p C_H (T_a - T) U \quad (4)$$

where C_p is specific heat of air at constant pressure, C_H is bulk sensible heat coefficient, T_a is air temperature, and T is surface temperature. Since sensible heat can be computed directly from the same mass transfer formulation and assumption (that the bulk evaporation coefficient is equal to the sensible heat coefficient) that is used to derive evaporation, the use of Bowen's ratio (which also is derived from this assumption) is unnecessary. In that regard, (4) now is used in place of (3).

Croley [1989a, b] tracked heat storage through the use of a point (zero areal dimension) superposition model of heat additions and losses. Heat storage in the lake is described now in terms of an assumed temperature profile superposition model to consider heat storage structure with lake depth and water temperature-depth profiles.

SUPERPOSITION HEAT STORAGE

Croley [1989a, b] applied the mixed-layer concept of others [Gill and Turner, 1976; Kraus and Turner, 1967] for the Great Lakes. To recapitulate, spring turnover (convective mixing of deep cold low-density water with cool high-density surface waters) occurs when surface temperature increases to 3.98°C, the temperature for maximum density of water. As water temperatures begin increasing above 3.98°C, surface temperature increases faster than temperatures at depth, until a stable temperature-depth profile develops with warmer, lower-density waters on top. As the net heat flux to the surface then changes to negative, surface temperature drops, and convective mixing keeps an upper layer at uniform temperature throughout (the "mixed layer"). The mixed layer deepens with subsequent heat loss until the temperature is uniform over the entire depth at 3.98°C, representing fall turnover. Then a symmetrical behavior is observed with temperatures less than 3.98°C as the lake continues to lose heat: the surface temperature drops the most until the net heat flux at the surface changes to positive again. Surface temperature then increases toward 3.98°C, and convective mixing forces uniform temperature at all depths, representing spring turnover.

Consider first the case of heat additions and losses for water temperatures above 3.98°C, after spring turnover has occurred. During the time (say 1 day) of a particular heat

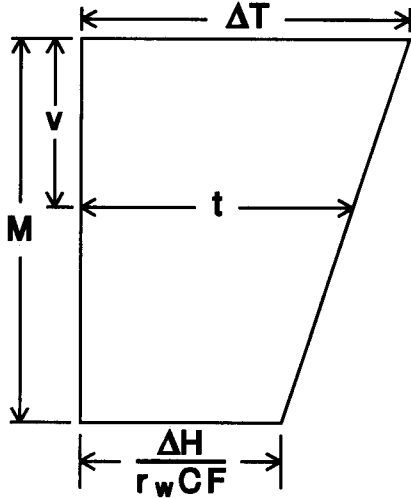


Fig. 1. Assumed temperature rise profile due to heat addition ΔH .

addition ΔH it penetrates a water volume M near the surface. This volume subsequently increases (deepens) with time as a function of conduction, diffusion, and mechanical mixing and is referred to as the "mixing volume" attributed to ΔH . As M deepens, in a sufficiently large lake, it approaches a limiting value since the effects of wind mixing at the surface diminish with distance from the surface. This limiting volume is referred to here as the "equilibrium volume" V_e . While M is increasing, ΔH mixes throughout M until, at some point, ΔH may become fully mixed. This volume ($M = F$) is called the "fully mixed" volume. If a fully mixed condition does occur at some point, then $F < V_e$.

As M grows from its initial value to F , the distribution of ΔH changes within M . The heat addition raises water temperatures, and the surface rise ΔT (associated with ΔH) decreases with increased mixing of ΔH throughout M and also with increases in M . The temperature rise at the bottom of the mixing volume, B , also would increase with the mixing of ΔH , but the increase in M would decrease it. Therefore B is taken as constant until ΔH is fully mixed throughout (and, at the same time, $M = F$). Thus B corresponds to the fully mixed condition ($M = F$) where the temperature rise at any depth, Δt , is constant throughout M : $\Delta t = \Delta T = B$ and $\Delta H = r_w C F B$. (Here r_w is the density of water and C is the specific heat of water.)

The water temperature increase Δt is taken as linear with volume v (measured down from the lake surface), from its maximum, $\Delta t = \Delta T$ at the surface ($v = 0$), to $\Delta t = B$ at the bottom of the mixing ($V = M$). By solving for B from the fully mixed condition, linear interpolation from $\Delta t = \Delta T$ at $v = 0$ to $\Delta t = B$ at $v = M$ gives

$$\Delta t = (\Delta T - B) \frac{M - v}{M} + B \quad (5)$$

as pictured in Figure 1, where $B = \Delta H / (r_w C F)$. Note that the assumed temperature rise profile (not the temperature profile) is assumed to be linear until the fully mixed condition obtains. This is not the same as assuming that the temperature profile is linear; indeed, the epilimnetic temperature

profile will be demonstrated to behave like the mixed layer model already discussed when comparisons are made to observed temperatures. Integrating the temperature increment over the profile with respect to volume gives

$$\Delta H = \int_0^M r_w C \Delta t \, dv = \frac{r_w C M}{2 - M/F} \Delta T \quad M < F \quad (6)$$

For $M \geq F$ the temperature rise profile remains uniform (fully mixed), and the water temperature increments decrease with increasing M :

$$\Delta H = r_w C M \Delta T \quad M \geq F \quad (7)$$

If the lake is sufficiently large ($V_c \geq V_e$, where V_c is the volume of the lake), then (6) and (7) apply. If, however, $F > V_e$ and the fully mixed condition is never reached ($M \leq V_e < F$ always), then of course only (6) applies. If the lake volume is reached before the limiting volume but after the fully mixed volume, then the actual mixing volume is constrained by the size of the lake and the water temperature increment is determined by the lake volume:

$$\Delta H = r_w C V_c \Delta T \quad F < V_c \leq M \quad (8)$$

where M is now the corresponding mixing volume in an unbounded lake. If the lake volume is reached before the fully mixed volume, then it is assumed that mixing continues, and the trapezoidal temperature profile approaches a rectangle as the bottom temperature B increases (since actual mixing volume is fixed), until the fully mixed condition is reached. Note, for $V_c \leq F$, that

$$\Delta H = \int_0^{V_c} r_w C \Delta t \, dv = \frac{1}{2} r_w C V_c (\Delta T + B) \quad (9)$$

If we assume that ΔT keeps changing as in (6), but B now increases as M increases (since the actual mixing volume cannot really increase), then by (6) and (9),

$$B = \left(\frac{2M}{2V_c - M V_c / F} - 1 \right) \Delta T \quad V_c \leq M \leq M_{(B = \Delta T)} \leq F \quad (10)$$

Actually, B increases until it is equal to ΔT , at which point the heat addition is fully mixed in the lake volume. From (10), with $B = \Delta T$,

$$M_{(B = \Delta T)} = \frac{2V_c}{1 + V_c / F} \quad (11)$$

Summarizing (6)–(11) and determining B similarly to ΔT , for $V_e < F \leq V_c$ or $V_e \leq V_c < F$ (i.e., $V_e < F$ and $V_e \leq V_c$),

$$\Delta T = \frac{2 - M/F}{r_w C M} \Delta H \quad (12)$$

$$B = \frac{1}{r_w C F} \Delta H \quad (13)$$

For $F \leq V_e \leq V_c$,

$$\Delta T = \frac{2 - M/F}{r_w CM} \Delta H \quad M < F \quad (14)$$

$$\Delta T = \frac{1}{r_w CM} \Delta H \quad F \leq M$$

$$B = \frac{1}{r_w CF} \Delta H \quad M < F$$

$$B = \frac{1}{r_w CM} \Delta H \quad F \leq M$$

For $F \leq V_c < V_e$,

$$\Delta T = \frac{2 - M/F}{r_w CM} \Delta H \quad M < F$$

$$\Delta T = \frac{1}{r_w CM} \Delta H \quad F \leq M < V_c \quad (16)$$

$$\Delta T = \frac{1}{r_w CV_c} \Delta H \quad V_c \leq M$$

$$B = \frac{1}{r_w CF} \Delta H \quad M < F$$

$$B = \frac{1}{r_w CM} \Delta H \quad F \leq M < V_c \quad (17)$$

$$B = \frac{1}{r_w CV_c} \Delta H \quad V_c \leq M$$

For $V_c < F \leq V_e$ or $V_c < V_e < F$ (i.e., $V_c < F$ and $V_c < V_e$),

$$\Delta T = \frac{2 - M/F}{r_w CM} \Delta H \quad M < \frac{2V_c}{1 + V_c/F} \quad (18)$$

$$\Delta T = \frac{1}{r_w CV_c} \Delta H \quad \frac{2V_c}{1 + V_c/F} \leq M$$

$$B = \frac{1}{r_w CF} \Delta H \quad M < V_c$$

$$B = \left(\frac{2M}{2V_c - MV_c/F} - 1 \right) \frac{2 - M/F}{r_w CM} \Delta H \quad (19)$$

$$V_c \leq M < \frac{2V_c}{1 + V_c/F}$$

$$B = \frac{1}{r_w CV_c} \Delta H \quad \frac{2V_c}{1 + V_c/F} \leq M$$

As time increases, the surface temperature increment on day j attributable to a past heat addition on day m , $\Delta T_{j,m}$, decreases, since the heat added on day m , ΔH_m , mixes throughout an enlarging mixing volume. Assume the mixing volume size $M_{j,m}$ is a function of accumulated wind movement from day m through day j . Thus only wind stirring

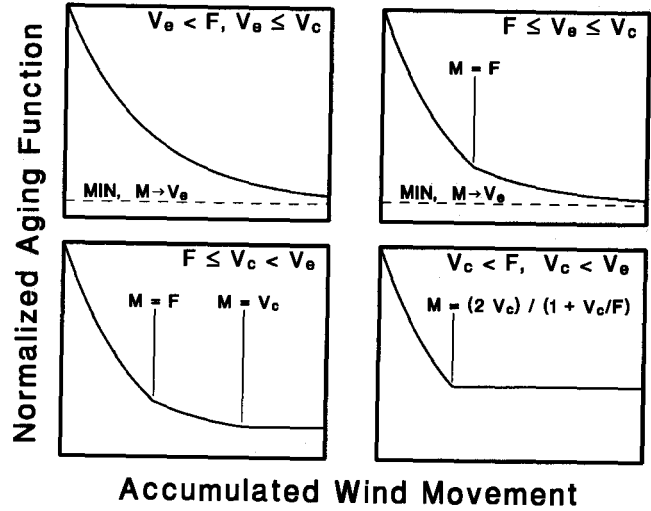


Fig. 2. Normalized aging function, $r_w CV_e \Delta T / \Delta H$, as a function of accumulated wind movement.

(mixing) events (and, to a lesser extent, time) are considered here for mixing. There should be some nonzero volume for no accumulated wind movement (accumulated wind movement equals zero), and the mixing volume should approach the limiting equilibrium volume V_e (in a sufficiently large lake) as the accumulated wind movement increases. Two such exponential functions are

$$M_{j,m} = V_e \left[1 - a^* \exp \left(-b^* \sum_{k=m}^j w_k \right) \right] \quad (20)$$

$$M_{j,m} = V_e \left[1 + a \exp \left(-b \sum_{k=m}^j w_k \right) \right]^{-1} \quad (21)$$

where w_k is the average daily wind speed across the lake on day k , and a and b are empirical parameters. Note that both functions satisfy the above limit requirements; the second formulation is found empirically to give superior results.

Combining (12), (14), (16), and (18) with (21), we have

$$\Delta T_{j,m} = f_{j,m} \Delta H_m \quad (22)$$

where $f_{j,m}$ can be interpreted as an "aging function,"

$$f_{j,m} = \frac{2 - M_{j,m}/F}{r_w CM_{j,m}} \quad M_{j,m} < \min \left(F, \frac{2V_c}{1 + V_c/F} \right)$$

$$f_{j,m} = \frac{1}{r_w CM_{j,m}} \quad (23)$$

$$\min \left(F, \frac{2V_c}{1 + V_c/F} \right) \leq M_{j,m} < \max \left(V_c, \frac{2V_c}{1 + V_c/F} \right)$$

$$f_{j,m} = \frac{1}{r_w CV_c} \quad \max \left(V_c, \frac{2V_c}{1 + V_c/F} \right) \leq M_{j,m}$$

The aging function $f_{j,m}$ is pictured conceptually in Figure 2 for different values of F and V_c . For recent heat additions, accumulated wind movement is low, the heat has penetrated little and is close to the surface, and it has a large influence

on surface temperature increments with a correspondingly high value for the aging function. As the accumulated wind movement increases, the aging function approaches the completely mixed limit(s) in (23).

Combining (13), (15), (17), and (19), with (21), we also have

$$B_{j,m} = g_{j,m} \Delta H_m \quad (24)$$

where $B_{j,m}$ corresponds to $\Delta T_{j,m}$ (as B does to ΔT) and $g_{j,m}$ is likewise:

$$g_{j,m} = \frac{1}{r_w C F} \quad M_{j,m} < \min(F, V_c)$$

$$g_{j,m} = \left(\frac{2M_{j,m}}{2V_c - M_{j,m}V_c/F} - 1 \right) \frac{2 - M_{j,m}/F}{r_w C M_{j,m}}$$

$$\min(F, V_c) \leq M_{j,m} < \min\left(F, \frac{2V_c}{1 + V_c/F}\right)$$

$$g_{j,m} = \frac{1}{r_w C M_{j,m}} \quad (25)$$

$$\min\left(F, \frac{2V_c}{1 + V_c/F}\right) \leq M_{j,m} < \max\left(V_c, \frac{2V_c}{1 + V_c/F}\right)$$

$$g_{j,m} = \frac{1}{r_w C V_c} \quad \max\left(V_c, \frac{2V_c}{1 + V_c/F}\right) \leq M_{j,m}$$

and from (5) the temperature rise anywhere in the mixing volume is

$$\Delta t_{j,m}(v) = (\Delta T_{j,m} - B_{j,m}) \frac{M_{j,m} - v}{M_{j,m}} + B_{j,m}$$

$$0 \leq v \leq \min(M_{j,m}, V_c)$$

$$\Delta t_{j,m}(v) = 0 \quad \min(M_{j,m}, V_c) < v \leq V_c \quad (26)$$

It is convenient to define the day when turnover occurs as day 0 since initial conditions are known then. The lake is 3.98°C throughout, and the heat in storage H_0 is $[r_w C V_c 3.98^\circ\text{C}]$. The heat in storage at the end of day m , H_m , becomes, for the case of continuous heat additions,

$$H_m = H_0 + \sum_{k=1}^m \Delta H_k \quad (27)$$

Temperature increments from past heat additions are added by superimposing the effects of past heat additions onto H_0 to determine the surface temperature:

$$T_j = 3.98^\circ\text{C} + \sum_{m=1}^j \Delta T_{j,m} \quad (28)$$

where T_j is the surface temperature at the end of day j . Likewise, in general, the temperature at depth (volume v) at the end of day j , $t_j(v)$, is

$$t_j(v) = 3.98^\circ\text{C} + \sum_{m=1}^j \Delta t_{j,m}(v) \quad 0 \leq v \leq V_c \quad (29)$$

For the case of continuous heat additions, (28) and (22) and repeated application of (27) give

$$T_j = 3.98^\circ\text{C} + \sum_{m=1}^j f_{j,m}(H_m - H_{m-1}) \quad (30)$$

If heat is removed, it comes from the surface layers, lowering surface and near-surface temperatures and resulting in convective mixing (lower-density waters at depth rise) and a deepening of the mixed layer. The least-mixed heat additions are removed first since they are most available for release (they are less distributed with depth than older additions and have their major fraction closest to the surface). Thus if heat now is removed after past continuous additions, such that the current heat in storage H_j drops below an earlier value H_p ($p < j$) but is greater than or equal to H_{p-1} ($H_{p-1} \leq H_j < H_p$), then the heat loss $H_{j-1} - H_j$ is regarded as coming from the intermediate heat additions (given by expanding $H_{j-1} - H_j$):

$$H_{j-1} - H_j = (H_{j-1} - H_{j-2}) + (H_{j-2} - H_{j-3})$$

$$+ \cdots + (H_{p+1} - H_p) + (H_p - H_j) \quad (31)$$

By eliminating these heat additions, (30) becomes

$$T_j = 3.98^\circ\text{C} + \sum_{m=1}^{p-1} f_{j,m}(H_m - H_{m-1}) + f_{j,p}(H_j - H_{p-1}) \quad (32)$$

Equivalently, we could define a new set of variables for heat additions: $(H'_m - H'_{m-1})$, $m = 1, \dots, j$, where

$$H'_m - H'_{m-1} = H_m - H_{m-1} \quad 1 \leq m < p$$

$$H'_m - H'_{m-1} = H_j - H_{p-1} \quad m = p \quad (33)$$

$$H'_m - H'_{m-1} = 0 \quad p < m \leq j$$

and (32) becomes

$$T_j = 3.98^\circ\text{C} + \sum_{m=1}^j f_{j,m}(H'_m - H'_{m-1}) \quad (34)$$

which is identical in form to (30). By using (27) applied to H'_m and $\Delta H'_m (= H'_m - H'_{m-1})$, (33) becomes

$$H'_m = H_m \quad 1 \leq m < p \quad (35)$$

$$H'_m = H_j \quad p < m \leq j$$

or

$$H'_m = \min(H_m, H_{m+1}, \dots, H_{j-1}, H_j) \quad (36)$$

and (34) can be written

$$T_j = 3.98^\circ\text{C} + \sum_{m=1}^j f_{j,m} \left(\min_{m \leq n \leq j} H_n - \min_{m-1 \leq n \leq j} H_n \right) \quad (37)$$

where

$$\min_{m \leq n \leq j} H_n = \min (H_m, H_{m+1}, \dots, H_{j-1}, H_j) \quad (38)$$

which avoids defining a new set of variables every time we have a heat loss and which is equivalent to (30) for the case of continuous heat additions. More generally, heat is added, then removed, then added, and so forth, and while recent additions may be lost, new additions will occur. Equation (37) applies for this universal case, in which heat additions and losses may follow one another.

Note that if for some index p

$$M_{j,p} \geq \max \left(V_c, \frac{2V_c}{1 + V_c/F} \right)$$

then, from (23),

$$f_{j,m} = f_{j,p}, \quad m = 1, \dots, p \quad (39)$$

Thus early terms with constant aging function values (say the first p terms) can be combined into a single term, and the j summation terms in (37) may be replaced with $j - p + 1$ terms:

$$\begin{aligned} T_j &= 3.98^\circ\text{C} + f_{j,p} \sum_{m=1}^p \left(\min_{m \leq n \leq j} H_n - \min_{m-1 \leq n \leq j} H_n \right) \\ &+ \sum_{m=p+1}^j f_{j,m} \left(\min_{m \leq n \leq j} H_n - \min_{m-1 \leq n \leq j} H_n \right) \\ &= 3.98^\circ\text{C} + f_{j,p} \left(\min_{p \leq n \leq j} H_n - H_0 \right) \\ &+ \sum_{m=p+1}^j f_{j,m} \left(\min_{m \leq n \leq j} H_n - \min_{m-1 \leq n \leq j} H_n \right) \quad (40) \end{aligned}$$

Equation (40) then may be rewritten by reassigning indices so that it is continuous over the dropped terms (1 through p are combined into term 1, $p + 1$ becomes 2, $p + 2$ becomes 3, \dots , and j becomes $j - p + 1 = i$), as follows:

$$T_i = 3.98^\circ\text{C} + \sum_{m=1}^i f_{i,m} \left(\min_{m \leq n \leq i} H_n - \min_{m-1 \leq n \leq i} H_n \right) \quad (41)$$

which is the same as (37). Note that the index does not really correspond to the number of days since the turnover, but it actually corresponds to the number of most recent days over

which the corresponding mixing volume in an unbounded lake is less than or equal to $\max [V_c, (2V_c)/(1 + V_c/F)]$.

Now consider the case of heat additions and losses for water surface temperatures below 3.98°C , after fall turnover has occurred. Equations (21)–(26) apply equally well for heat and temperature decrements as for increments (since water is most dense at 3.98°C), with $M_{j,m}$ and $f_{j,m}$ given in terms of parameters that apply for this time of the year; replace a and b in (21) with a' and b' and replace F in (23) and (25) with F' .

Likewise, (27)–(30) are valid for the case of continuous heat losses. If heat is added, it is added to the surface layers, raising surface and near-surface temperatures and resulting in convective mixing and a deepening of the mixed layer. In fact, this case is symmetrical to the discussion of heat losses after the spring turnover, preceding (31). The least-mixed heat losses are compensated first since they are most available for amelioration. The heat addition $H_{j-1} - H_j$ is regarded as going to the intermediate heat deficiencies given by expanding $H_{j-1} - H_j$ as in (31), which again results in (32)–(41), where a , b , and F are replaced by a' , b' , and F' . Thus computer code for the equations above may be used for both cases (postspring turnover and postfall turnover) where the appropriate empirical values are used (a , b , and F or a' , b' , and F' , respectively).

Each day i , (41) is used (with a , b , and F or a' , b' , and F' , as appropriate) to compute temperature T_i as a function of H_i in heat balance, heat storage, and evaporation calculations, and when the point (T_i, H_i) then is determined, index adjustments are made to account for combined early terms (as in (40) and (41)). When (T_i, H_i) approaches $(3.98^\circ\text{C}, H_0)$, the number of summation terms in (41) approaches zero until at this point there are no summation terms in (41). Then as (T_i, H_i) departs from $(3.98^\circ\text{C}, H_0)$, the number of summation terms in (41) begins to grow again. Furthermore, as (T_i, H_i) passes through $(3.98^\circ\text{C}, H_0)$, either from greater than to less than or vice versa, the appropriate empirical parameters (a , b , and F or a' , b' , and F') are switched, as this represents a turnover of the water column.

Equations (5)–(41) above replace (15)–(21) given by Croley [1989a] and (20)–(28) given by Croley [1989b]; equation (4) above replaces (26) and (32) given by Croley [1989a] and (34), (35), and (41) given by Croley [1989b].

APPLICATION

Calibration

Meteorology data for 1948–1985 and water surface temperature data on each of the Great Lakes, except Lake Michigan, were taken and prepared as described by Croley [1989a, b] and extended to 1988. Water surface temperature data for Lake Michigan from 1981 through 1985 were gleaned from areal maps prepared at the National Weather Service's Marine Predictions Branch (B. Newell, personal communication, 1990). The heat balance model presented by Croley [1989a, b], with the superposition heat storage model given here, was calibrated to determine values of the eight parameters (a , b , F , a' , b' , F' , V_e , and p) that give the smallest sum-of-squared-errors between model and actual daily surface temperatures by using methods described elsewhere [Croley and Hartmann, 1984]. (The eighth parameter, p , is

TABLE 1. Daily Calibration Results at the Great Lakes

	Superior	Michigan	Huron	St. Clair	Erie	Ontario
Surface area, km ²	82,100	57,800	59,600	1,114	25,700	18,960
Volume, km ³	12,100	4,920	3,540	3.3	484	1,640
Average depth, m	147	85.1	59.4	3.05	18.8	86.5
<i>Calibrated Parameter Values</i>						
<i>a</i>	$6.288 \times 10^{+0}$	$7.290 \times 10^{+0}$	$6.000 \times 10^{+0}$	0	$3.093 \times 10^{+0}$	$7.710 \times 10^{+0}$
<i>b</i> , m ⁻¹ s	3.300×10^{-3}	2.600×10^{-3}	2.200×10^{-3}	0	5.213×10^{-3}	2.800×10^{-3}
<i>F</i> , km ³	$3.299 \times 10^{+3}$	$5.100 \times 10^{+2}$	$4.288 \times 10^{+3}$	$3.300 \times 10^{+0}$	$1.000 \times 10^{+2}$	$2.000 \times 10^{+2}$
<i>a'</i>	$1.800 \times 10^{+0}$	$1.199 \times 10^{+0}$	$7.699 \times 10^{+0}$	0	$2.710 \times 10^{+0}$	$3.597 \times 10^{+0}$
<i>b'</i> , m ⁻¹ s	3.390×10^{-3}	2.302×10^{-3}	5.100×10^{-3}	0	5.462×10^{-3}	4.898×10^{-3}
<i>F'</i> , km ³	$4.972 \times 10^{+3}$	$4.000 \times 10^{+3}$	$1.500 \times 10^{+3}$	$3.300 \times 10^{+0}$	$1.000 \times 10^{+2}$	$4.300 \times 10^{+2}$
<i>V_e</i> , km ³	$1.200 \times 10^{+4}$	$5.000 \times 10^{+3}$	$9.990 \times 10^{+3}$	$3.300 \times 10^{+0}$	$8.500 \times 10^{+2}$	$2.001 \times 10^{+3}$
<i>p</i>	1.300	1.070	1.180	1.191	1.288	1.219
<i>Calibration Period Statistics (1979–1988)^a</i>						
Number of observations	170	137	229	64	237	284
Means ratio ^b	1.004	1.008	0.997	1.121	1.029	1.018
Variations ratio ^c	1.001	0.899	1.004	1.762	1.136	0.980
Correlation ^d	0.977	0.972	0.984	0.964	0.988	0.982
rms error ^e	1.180	1.558	1.253	4.000	1.510	1.367
<i>Verification Period Statistics (1966–1978)</i>						
Number of observations	94		150		104	149
Means ratio ^b	0.916		1.001		1.047	0.979
Variations ratio ^c	1.043		0.958		1.174	0.942
Correlation ^d	0.952		0.977		0.978	0.968
rms error ^e	1.384		1.304		1.800	1.737
<i>Combined Period Statistics (1966–1988)</i>						
Number of observations	264	137	379	64	341	433
Means ratio ^b	0.972	1.008	0.999	1.121	1.035	1.006
Variations ratio ^c	1.011	0.899	0.990	1.762	1.145	0.973
Correlation ^d	0.970	0.972	0.982	0.964	0.985	0.978
rms error ^e	1.256	1.558	1.274	4.000	1.604	1.504

^aData between January 1, 1979 and August 31, 1988 for all Great Lakes and between January 1, 1981 and November 30, 1985 for Lake Michigan.

^bRatio of mean model surface temperature to data mean.

^cRatio of variance of model surface temperature to data variance.

^dCorrelation between model and data surface temperature.

^eRoot-mean-square error between model and data surface temperatures in degrees Celsius.

an empirical coefficient that reflects the effect of cloudiness on the atmospheric net longwave radiation exchange; see Croley [1989a, b]). Calibrations were performed over the last few data-rich years, 1978–1988 and were verified by comparison with the earlier years (1965–1977). No data were used until 1980 in the calibrations to allow sufficient initialization; that is, the 1978–1980 period was used to initialize the model prior to calibration data beginning in 1980, from arbitrary initial conditions in 1978. Table 1 summarizes calibration results (and replaces Table 3 given by Croley [1989a] and Table 4 given by Croley [1989b]).

The goodness of fit statistics for the calibration and verification periods in Table 1 show generally good agreement on the deep lakes between the actual and calibrated model surface temperatures; correlations are high, and means and variances are close between the data and model for each lake. The root mean square errors are 1.2°C–1.6°C. In all cases, except Lake St. Clair, the results are superior to the earlier effort by Croley [1989a, b]; the most dramatic improvement is on Lake Erie. The effect of the bottom of Lake Erie on the growth of the mixing layer is now explicitly considered; this was not possible with the previous deep water heat storage model [Croley, 1989a, b]. The Lake St. Clair application remains poor because the dynamics of that lake are poorly represented by the heat storage model since

advected heat is large and unknown; the thermodynamics of the entire river on which relatively small Lake St. Clair sits must be considered to properly estimate the heat balance and heat storage. Other observations on the calibration of the model mirror those presented earlier [Croley, 1989a, b].

Thermal Structure

It is possible to compute water temperature-depth profiles (as well as surface temperatures) from (22), (24), (26), and (29) with knowledge of the depth-volume relationship for the lake in question. This enables comparison of model outputs to temperature profile data as well as to surface temperatures. To demonstrate the physical adequacy of the conceptual model, mixed layer development and turnovers were illustrated (see first paragraph of the section entitled Superposition Heat Storage) by plotting the model output of water temperature at depth for Lake Superior from 1948 through 1988, as exemplified in Figure 3 for 1976. (This year was selected since it was a particularly data-rich year in terms of bathythermograph data, discussed shortly.) Figure 3 is a plot of depth-temperature profiles every 20 days and reveals the development of the mixed layer after the "spring turnover" in June (normal late-in-the-year occurrence for northerly and large Lake Superior). As surface temperature begins to

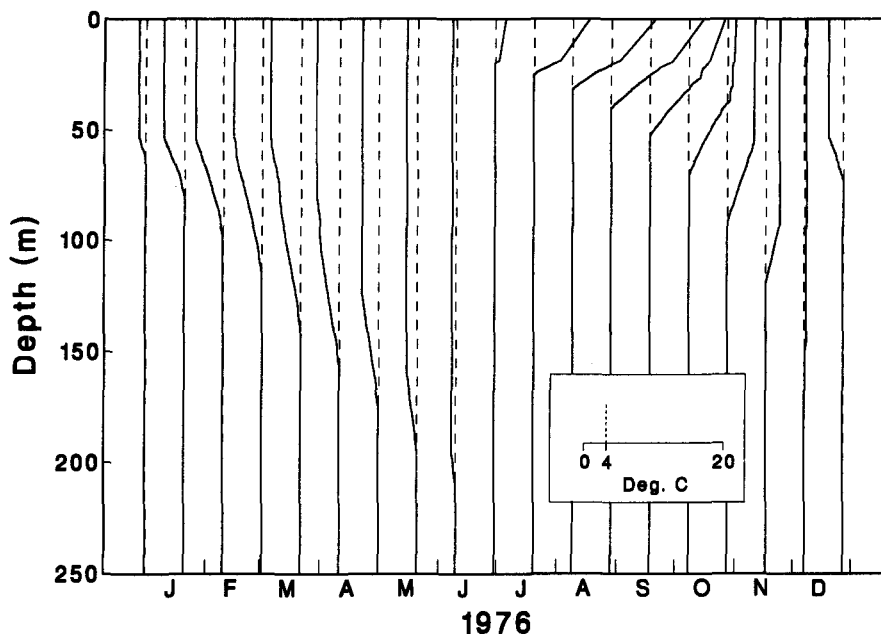


Fig. 3. 1976 Lake Superior model 20-day depth-temperature profiles.

climb with heat additions from June through August, temperatures at depth rise, the depth of the heat addition increases, and a well-defined mixed layer develops. These developments continue as heat is lost and surface temperatures drop from August through December. The mixed layer deepens as convective mixing takes place with the lowering of surface temperature, and the temperature profile approaches a vertical line corresponding to 3.98°C at turnover in mid-December. The symmetrical development after the "fall turnover" is illustrated in the first half of Figure 3.

Averaged bathythermograph data from Lake Superior for 1972–1979 [Assel, 1983b, 1985] are available from ship crossings, and these data were plotted coincident with model results,

as exemplified in Figure 4 for 1976, the year which had the most data. In general, these plots revealed that the model underpredicted the maximum depth of heat loss after fall turnovers (in the winter). This is depicted in Figure 4 for the January through April period. For the postspring turnovers (in the summer and fall) the depth of heat penetration is fairly well predicted, as seen in Figure 4 for the August through December period. Throughout the entire year, and particularly after the spring turnover, temperatures were judged to match fairly well, and turnover timing was felt to be very good. These data comparisons represent use of completely independent data; they were not used in any way in calibrating the model, although they did suggest the concepts for the dynamics of the situation.

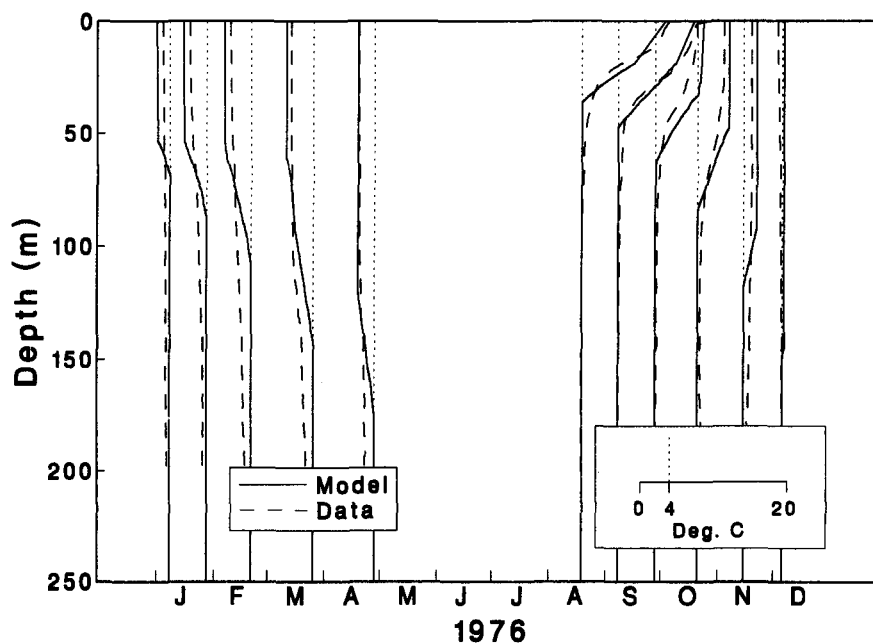


Fig. 4. 1976 Lake Superior bathythermograph and model depth-temperature profile comparisons.

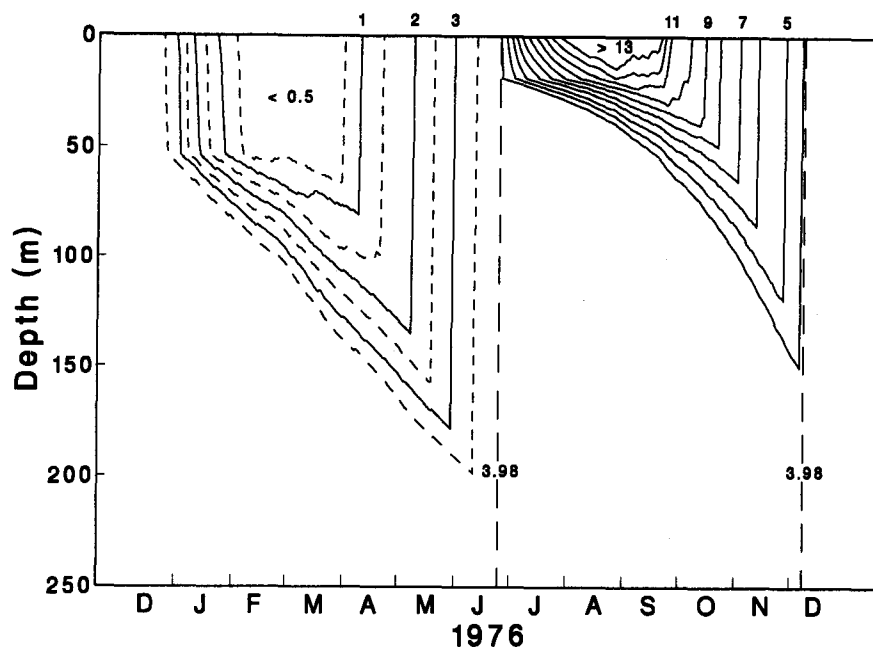


Fig. 5. 1976 Lake Superior model lake-wide-averaged vertical temperature distribution.

As another effort to compare with independent data, isolines of selected temperatures at depth throughout the year were constructed to compare with available studies for Lake Superior. Figure 5 depicts the lake-wide-averaged vertical distribution of temperature in Lake Superior for 1976. The semiannual alternation between periods of stratification and extensive vertical mixing, typical of dimictic lakes, is well illustrated and agrees quite well with the seasonal cycle depicted in like manner by Bennett [1978, p. 314]. As he pointed out, "winter stratification is weaker than summer stratification because water temperature cannot be less than 0°C and hence, strong vertical density gradients cannot develop during the winter." The mixed layer during the winter is deeper than during the summer, and the downward penetration of isotherms is greater. His other observations on depth of mixing and stratification for Lake Superior are also found in the model outputs. While Bennett observes that the initial depth of the epilimnion in late June to mid-July is about 10 m, Figure 3 shows about 20 m, which is typical of the model outputs for other years. However, he reports that the epilimnion depth increases to about 145 m typically at the end of November, which is consistent with the model outputs. He reports that the epilimnion begins at about 40 m in early January after fall turnover and increases to 250 m or more by early June; this agrees closely with the model outputs as reflected in Figures 3, 4, and 5.

Finally, to illustrate the heating cycle of Lake Superior further, Figures 6 and 7 depict the heat in storage plotted against time (Figure 6) and water surface temperature (Figure 7) for 1976. Both show an anomalous perturbation on May 1, which is a result of the empirical ice cover function that is defined only from December through April. These figures provide a good depiction of the hysteresis that exists. Spring turnover occurs in mid-June, and water surface temperature and heat in storage increase until mid-August. Then water surface temperature begins dropping while total heat in storage is still increasing, as heat moves from the

surface downward. In mid-September, heat in storage also starts dropping with water surface temperature, although at a smaller absolute rate with temperature than the earlier rise. Turnover occurs in mid-December as the curve in Figure 7 again passes through the same point (3.98°C, 0.482×10^{20} cal) as the other turnover. There is a similar asymmetrical behavior after this turnover, but the storage characteristics are different because of the weakened mixing mechanisms that exist with temperature range limitations in the winter-time, as mentioned previously in connection with Figures 3 and 5.

Evaporation Occurrence Structure

The thermodynamics and heat storage superposition model may be used for estimating lake evaporation. Com-

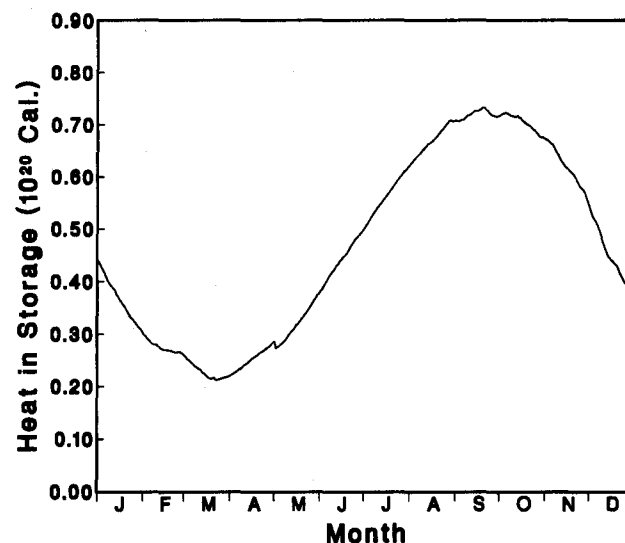


Fig. 6. Seasonal variation of 1976 Lake Superior total heat storage.

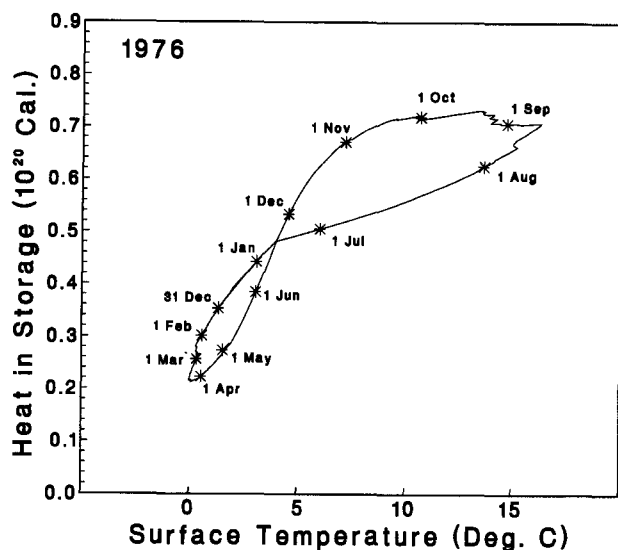


Fig. 7. Variation of 1976 Lake Superior total heat storage with surface temperature.

Comparisons of heat fluxes and evaporation estimates between an earlier version of this model and other researchers are available elsewhere [Croley, 1989a, b]. The superposition model resulted in further improvements in the comparisons, but they were not sufficiently different to warrant presenting again here. However, investigation of the structure of occurrence of evaporation and of the sensitivity of evaporation to initial heat storage conditions were not considered. This subsection considers the former, and the subsequent subsection considers the latter.

Quinn and den Hartog [1981] noted, in their studies on Lake Ontario during the International Field Year on the Great Lakes, that evaporation events can take place in which a majority of annual evaporation occurs within a few days. They noted also that this appeared to be the case on Lake Superior. While actual evaporation is unknown, by estimating the evaporation time series on each lake it is possible to address the question, To what extent is evaporation an event-oriented process? Inspection of time series of meteorology and estimated evaporation on all of the Great Lakes for the period 1948–1988, as exemplified in Figure 8 for Lake Superior for July 1975 through June 77, illustrates the nature of the process.

Significant evaporation on Lake Superior begins in August and continues through April (evaporation is generally July through March on the other Great Lakes except Lake Erie where ice cover restricts significant evaporation to July through December or January). During this period, lake evaporation appears to be highly variable, depending to a large extent on wind speed. Individual daily estimated evaporation peaks often do correspond to daily wind speed peaks, but the extent of this correspondence is seen to change during the evaporation season. While wind speed fluctuates daily about an underlying constant during the period September through March on Lake Superior, estimated evaporation fluctuates daily like wind speed but generally increases from September through December and then generally decreases; see Figure 8. As wind speed increases and humidity drops during the fall and early

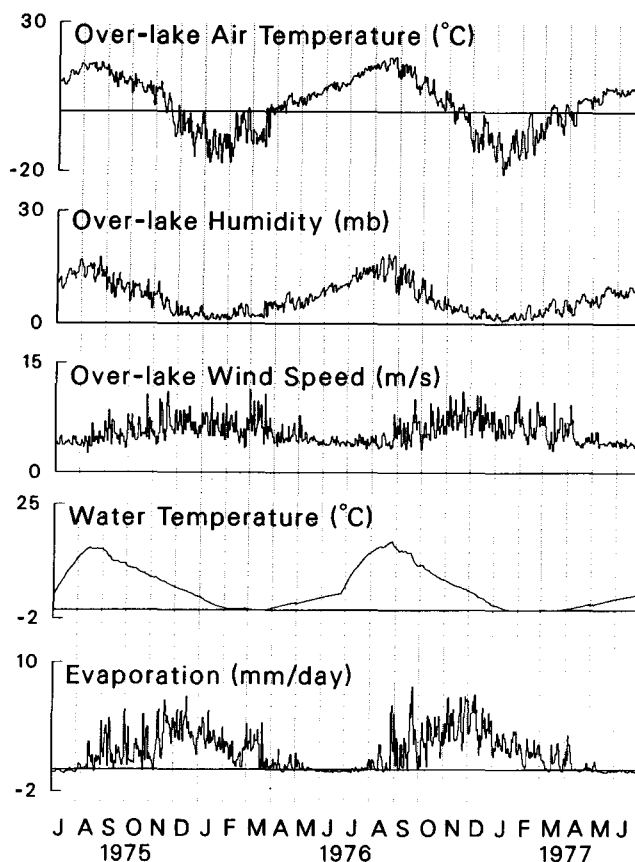


Fig. 8. 1975–1977 annual cycles of average Lake Superior meteorology and evaporation.

winter, estimated evaporation increases. Then, dropping water temperatures lower the vapor deficit over water, and estimated evaporation generally drops during late winter and spring. Superimposed on this general behavior are the fluctuations corresponding to changes in wind speed and humidity that are associated with the passage of air masses. Thus evaporation may be separated into two components: a steady component rising and falling throughout the fall and winter and a highly variable component corresponding to passage of individual air cells (events).

Inspection of the 41-year simulations for each of the Great Lakes reveals that over a third of the estimated annual evaporation occurs in less than a tenth of the annual cycle (not necessarily continuously). Two thirds occur in about one quarter of the annual cycle. The complete spectrum of occurrences of estimated annual evaporation fractions on Lake Superior are summarized in Figure 9 where, for example, one may estimate that 50% of the annual evaporation occurs in 17% of the annual cycle. Table 2 summarizes these statistics for other Great Lakes.

It is very important to note that the time occurrence structure of evaporation events is dependent upon the nature of air mass and frontal movements in the atmosphere over the Great Lakes. Any study of an altered atmosphere must consider changes in the occurrence structure of driving events and not simply changes in general meteorological variable values. For example, a recent Environmental Protection Agency study of climate change impacts [U.S. Environmental Protection Agency, 1989] directed scientists to

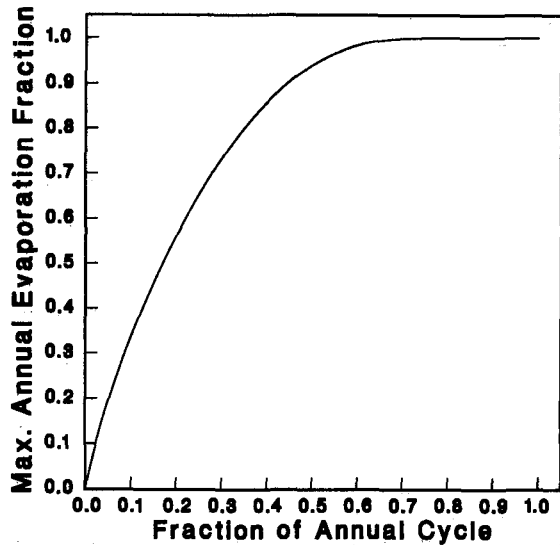


Fig. 9. Lake Superior maximum estimated possible evaporation during fractions of the annual cycle.

consider general circulation model (GCM) outputs for a simulation of $2 \times \text{CO}_2$ in the atmosphere by changing all meteorological values in their historical data sets by the same relative amounts as observed between $1 \times \text{CO}_2$ and $2 \times \text{CO}_2$ GCM simulations [Croley, 1990]. However, this resulted in the historical sequence of events unchanged; time occurrences remained the same and only the magnitude of events was modified for subsequent hydrology simulations. The nature of the time occurrence structure for lake evaporation suggests that evaporative losses are sensitive also to shifts in the timing of air mass movements that may occur with climate change, as well as to general changes in meteorology.

Thermal Dynamics

Simulation experiments were designed to look at Great Lakes thermal behavior and to answer some specific questions. For example, heavy lake effect snowfalls are expected after a very warm summer. The reasoning is that with a very warm lake, wintertime evaporation will be above normal, and the air masses reaching the lee side of a lake will have more moisture to release as it cools over land. However, in these situations, the snowfall never seems to be as heavy as

TABLE 2. Minimum Fractions of the Year for Occurrence of Estimated Annual Evaporation Fractions

Annual Evaporation Fraction, %	Lake Superior, %	Lake Michigan, %	Lake Huron, %	Lake Erie, %	Lake Ontario, %
5	1.0	1.0	1.0	1.0	1.0
10	2.3	2.2	2.2	2.1	2.2
20	5.2	5.1	5.0	5.0	5.1
33.3	9.9	9.8	9.5	9.4	9.8
50	17.0	17.1	16.4	16.6	16.8
66.7	25.8	26.3	25.4	26.3	25.8
80	35.0	36.1	35.4	37.5	35.4
90	44.5	46.6	46.4	50.2	45.8
95	51.6	54.8	54.7	60.0	54.0
100	74.8	81.5	82.0	88.3	81.7

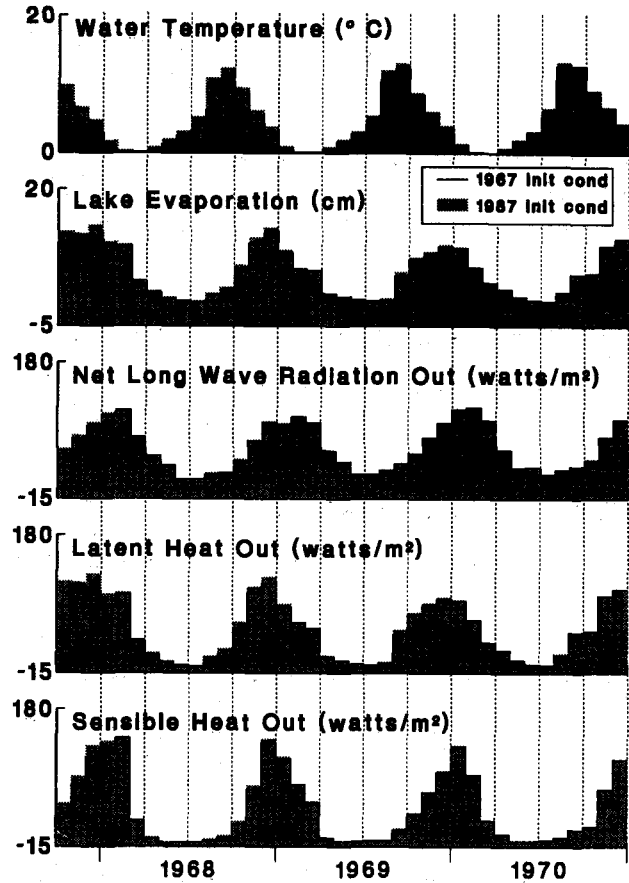


Fig. 10. 1967–1970 Lake Superior temperature and heat flux comparisons for small and large heat storage initial conditions.

expected, and model simulations were used to find out why and where additional heat goes if not into evaporation. A related question is, What difference does different initial conditions on heat content of the lake make on the state of the lake several months later? The experiment consisted of using several years of meteorology with different peak heat storage amounts as initial conditions and inspecting the resulting evaporation and heat flux realizations.

The time series realization of daily total heat in Lake Superior for 1948–1988 was inspected to identify the date and amount of the annual peak heat in storage in the lake for each year of record. The smallest peak heat in storage of 0.61×10^{20} cal occurred on October 4, 1967, and the largest of 0.79×10^{20} cal occurred on September 29, 1987. It appeared that an even higher one would occur in 1988, but the record stops at the end of August 1988. Both 1987 and 1988 are part of the recent hot drought. The meteorology of October 5, 1967 through December 31, 1970 was used in two simulations beginning with the two heat storage structures on the above two dates. These represent the extreme heat storages of record in Lake Superior, and comparison of the outputs illustrates the effect of initial conditions on the lake heat balance and the atmosphere. Monthly outputs are summarized in Figure 10 for both simulations.

The effect of the higher-heat initial condition is to increase the seasonal peak monthly overlake air temperature in September or October in the next 2 years by about 1°C and in 1970 by about 0.6°C ; however, the August–April evapo-

ration season overlake air temperature increase is about 0.5°C in the remainder of the 1967–1968 season, 0.6°C in the 1968–1969 season, and 0.2°C in 1969–1970. Other overlake meteorology is only slightly affected. The peak monthly (September) water surface temperature is increased by about 2.7°C (1967), 2.0°C (1968), 0.7°C (1969), and 0.2°C (1970), while the evaporation season increase is about 1.2°C (1967–1968), 1.1°C (1968–1969), and 0.4°C (1969–1970). The evaporation peak in December is increased by 2.7 cm or 25% (1967), 1.0 cm or 8% (1968), 0.3 cm or 3% (1969), and 0.1 cm or 1% (1970), while the evaporation season increase is about 12.4 cm or 25% (1967–1968), 6.1 cm or 13% (1968–1969), and 2.5 cm or 5% (1969–1970). The increase in total heat released (net longwave, latent, and sensible) during the year from August through July is 21 W m⁻² or 14% (1967–1968), 8 W m⁻² or 7% (1968–1969), and 3 W m⁻² or 3% (1969–1970). Of this, evaporation (latent heat release) accounted for 56% (12 W m⁻²), 50% (5 W m⁻²), and 60% (2 W m⁻²), respectively.

The increased heat in storage at the beginning of the simulation results in higher overlake air and water surface temperatures and is released through increases in net longwave radiation, sensible, and latent heat transfers. The effect of the change in initial conditions is seen to have an effect 3 years later, but the initial condition change considered here is extreme. One may expect that the effect of initial conditions, while dependent on their magnitude, lasts between 1 and 3 years. Heat release does not all occur in the first evaporation season; the release increased only by about 14% in the first 10 months (representing only about 60% of the total increase to occur in all remaining months), and only about half of that was increased evaporation. The other half of the additional heat release was accomplished through sensible and longwave radiation increases. This further suggests that the atmosphere above and downwind of the lake surface, while containing more moisture from lake evaporation, also contains more heat; the air temperature is higher and the lower layer of the atmosphere may cool without necessarily losing more moisture in the form of increased snowfall. Thus while evaporation may increase significantly after a warm summer, sensible and longwave radiation transfers also increase, and the extra heat is released over more than the next year. Lake effect snowfall may not increase significantly near the lake but may extend further from the lake as more overland cooling must take place as the air mass moves away from the lake to produce lake effect snowfall.

SUMMARY

A new heat storage superposition model is described that explicitly considers lake capacity and mixing capacity in temperature-depth profile development as a function of the wind aging of past heat additions. This superposition model extends the existing lumped-parameter thermodynamic model to lake depth, and recalibration yields improved matches to remotely sensed water surface temperatures on all of the Great Lakes as well as allowing further verification of temperature-depth profiles with independent bathythermograph data. This conceptual model depicts seasonal heating and cooling cycles, heat-temperature hysteresis, water column turnovers, and mixed-layer developments, in accordance with other investigators' physical models, while providing the capability for multiple, long-period, continuous simulations.

We can now look at continuous long-term dynamics of lake heating and evaporation; this enables further studies of climate change, water balances, groundwater, ice, lake effect snowfall, and other evaporation-dependent phenomenon. The time occurrence structure of evaporation on the Great Lakes suggests correspondence with air mass movements over the lakes; large amounts of the annual evaporation total appear to occur over small portions of the year on an event-oriented basis. This has significance for studies of changed atmospheres, such as in climate change impact studies. These studies must account for changes in the time occurrence of events as well as for general changes in meteorology. Of course, a more complete picture could be obtained if the lake dynamics were considered in conjunction with an appropriate mesoscale atmospheric model. Such a coupled model would be useful in a variety of other studies as well, including the assessment of the inducement of lake effect snowfall by large heat storage in the lakes.

While evaporation may increase significantly after a warm summer, sensible and longwave radiation transfers also increase, and the extra heat is released over more than the next year. Lake effect snowfall may not increase significantly near the lake but may extend further from the lake. In the absence of a coupled atmospheric-lake thermodynamic model, it still should be possible to look for changes in lake effect snowfall in conjunction with evaporation analyses from the lake. Extensive snow cover data bases are now in place for the Great Lakes, and it is often quite easy to identify lake effect snowfall about the lakes. By using peak heat storage estimates from the evaporation model to identify likely candidate years for altered lake effect snowfall patterns, searches of these data bases and display of snowfall patterns may reveal the coupling. Further analyses would be appropriate through couplings with mesoscale atmospheric models. Also, Lake Michigan and Erie are recognized to have significant lake effect snowfall amounts; joint evaporation modeling and snowfall data base searches (and atmospheric modeling) on these lakes may prove more fruitful than studies on Lake Superior.

Other areas for continued research on large-lake evaporation include the assessment of net groundwater fluxes between lakes, heretofore impossible since evaporation was estimated as a residual of lake water balances with groundwater assumed negligible. Groundwater can now be estimated as a residual in a water balance and compared between adjacent lakes. The next area for improvement of the large-lake evaporation models is the incorporation of a complete heat balance and mass balance for ice packs on the lakes, including related redevelopment of empirical ice cover functions. Such redevelopment can now include estimates of lake heat storage and surface heat fluxes as the ice cover functions are integrated with ice growth thermodynamics in the newly developing lake evaporation models.

REFERENCES

- Assel, R. A., A computerized ice concentration data base for the Great Lakes, *NOAA Data Rep. ERL GLERL-24*, Great Lakes Environ. Res. Lab., Natl. Oceanic and Atmos. Admin., Ann Arbor, Mich., 1983a.
- Assel, R. A., Lake Superior bathythermograph data: 1973–79, *NOAA Data Rep. ERL GLERL-25*, Great Lakes Environ. Res. Lab., Natl. Oceanic and Atmos. Admin., Ann Arbor, Mich., 1983b.

- Assel, R. A., Lake Superior cooling season temperature climatology, *NOAA Tech. Memo. ERL GLERL-58*, Great Lakes Environ. Res. Lab., Natl. Oceanic and Atmos. Admin., Ann Arbor, Mich., 1985.
- Atmospheric Environment Service, Monthly and annual evaporation from the Great Lakes bordering Canada, report, Environ. Canada, Downsview, Ont., 1988.
- Bennett, E. B., Characteristics of the thermal regime of Lake Superior, *J. Great Lakes Res.*, 4(3-4), 310-319, 1978.
- Croley, T. E., II, Verifiable evaporation modeling on the Laurentian Great Lakes, *Water Resour. Res.*, 25(5), 781-792, 1989a.
- Croley, T. E., II, Lumped modeling of Laurentian Great Lakes evaporation, heat storage, and energy fluxes for forecasting and simulation, *NOAA Tech. Memo. ERL GLERL-70*, Great Lakes Environ. Res. Lab., Natl. Oceanic and Atmos. Admin., Ann Arbor, Mich., 1989b.
- Croley, T. E., II, Laurentian Great Lakes double-CO₂ climate change hydrological impacts, *Clim. Change*, 17, 27-47, 1990.
- Croley, T. E., II, and H. C. Hartmann, Lake Superior basin runoff modeling, *NOAA Tech. Memo. ERL GLERL-50*, Great Lakes Environ. Res. Lab., Natl. Oceanic and Atmos. Admin., Ann Arbor, Mich., 1984.
- Derecki, J. A., Operational estimates of Lake Superior evaporation based on IFYGL findings, *Water Resour. Res.*, 17(5), 1453-1462, 1981.
- Gill, A. E., and J. S. Turner, A comparison of seasonal thermocline models with observation, *Deep Sea Res.*, 23, 391-401, 1976.
- Kraus, E. B., and J. S. Turner, A one-dimensional model of the seasonal thermocline, II, The general theory and its consequences, *Tellus*, 19, 98-105, 1967.
- McCormick, M. J., and G. A. Meadows, An intercomparison of four mixed layer models in a shallow inland sea, *J. Geophys. Res.*, 93(C6), 6774-6788, 1988.
- Phillips, W. D., Evaluation of evaporation from Lake Ontario during IFYGL by a modified mass transfer equation, *Water Resour. Res.*, 14(2), 197-205, 1978.
- Phillips, W. D., and J. G. Irbe, Land-to-lake comparison of wind, temperature, and humidity on Lake Ontario during the International Field Year for the Great Lakes (IFYGL), *Rep. CLI-2-77*, Atmos. Environ. Serv., Environ. Canada, Downsview, Ont., 1978.
- Pinsak, A. P., and G. K. Rodgers, Energy balance, in *IFYGL—The International Field Year For The Great Lakes*, edited by E. J. Aubert and T. L. Richards, pp. 169-197, National Oceanic and Atmospheric Administration, Ann Arbor, Mich., 1981.
- Quinn, F. H., An improved aerodynamic evaporation technique for large lakes with application to the International Field Year for the Great Lakes, *Water Resour. Res.*, 15(4), 935-940, 1979.
- Quinn, F. H., and G. den Hartog, Evaporation Synthesis, in *IFYGL—The International Field Year For The Great Lakes*, edited by E. J. Aubert and T. L. Richards, pp. 221-245, National Oceanic and Atmospheric Administration, Ann Arbor, Mich., 1981.
- Richards, T. L., and J. G. Irbe, Estimates of monthly evaporation losses from the Great Lakes, 1950-1968, based on the mass transfer technique, paper presented at the 12th Conference on Great Lakes Research, Int. Assoc. of Great Lakes Res., Ann Arbor, Mich., May 1969.
- Schertzer, W. M., Energy budget and monthly evaporation estimates for Lake Superior, 1973, *J. Great Lakes Res.*, 4(3-4), 320-330, 1978.
- Schertzer, W. M., Heat balance and heat storage estimates for Lake Erie, 1967 to 1982, *J. Great Lakes Res.*, 13(4), 454-467, 1987.
- U.S. Environmental Protection Agency, The potential effects of global climate change on the United States, Report to Congress, *Rep. EPA-230-05-89-050*, edited by J. B. Smith and D. A. Tirpak, EPA Office of Policy, Plann., and Eval., Washington, D. C., 1989.
- T. E. Croley, II, Great Lakes Environmental Research Laboratory, 2205 Commonwealth Boulevard, Ann Arbor, MI 48105.

(Received April 24, 1991;
revised September 17, 1991;
accepted September 26, 1991.)